CMOS-NANOWELL BASED HYBRID SMART BANDAGE FOR LONG TERM MONITORING OF WOUND HEALING VIA CYTOKINE QUANTIFICATION IN-SITU

Chengjie Zhu[1], Pengfei Xie[2], Ryan Thorpe[1], Jesus Maldonado[1], Suneel Kumar[2], Aaron Mazzeo[2], Mehdi Javanmard[2], Francois Berthiaume[2] and Kaushik Sengupta[1]
[1]Princeton University, NJ, USA
[2]Rutgers University, NJ, USA

ABSTRACT

Long-term monitoring of the chronic wound can allow autonomous wound healing. Prior attempts that sense wound closure dynamics in bandage forms are based on pressure, temperature and pH, lacking specific bio-molecular information that is critical for accurate acquisition of growth factors in various wound healing stages. This work presents a hybrid CMOS/nanowell co-design approach to target cytokine level to predict wound closure dynamics. The complete impedance spectroscopy chip is designed and fabricated in TSMC 65 nm LP process and is integrated on a flexible PCB compatible to "Smart Bandage" forms along with nanowell sensors located at the back and peripheral circuits. The proposed system demonstrates the sensitivity of IL-6 cytokine on the order of 100 pg/mL, and shows strong correlations to the standardized ELISA tests. This proposed CMOS/nano hybrid approach shows a path towards highly multiplexed and low-cost "Smart Bandages" for autonomous closed-loop wound monitoring and healing applications.

KEYWORDS

Smart bandages, cytokine, wound healing, impedance spectroscopy, nano-fabrication, ELISA.

INTRODUCTION

Over 6 million of people in US is currently living under complications resulting from unhealed chronic wounds. Long-term monitoring of chronic wounds, coupled with on-demand medication, could enable autonomous wound healing systems, thus paving the way towards patient-specific and wound-specific treatments that optimize the local immune and angiogenic responses, and eventual healing. Currently, the treatment of chronic wounds requires frequent visits to physicians and consecutive openings of the bandages for visual check. Unnecessarily disturbing the wound environment, and limiting wound evaluation to few observable features may contribute to slow healing and the risk of bacterial infection and sepsis [1]. The key technology to minimize the risks is to enable point-of-care diagnostic devices in compact packages, based on integrated circuit technology, such as CMOS (complementary-metal-oxide-semiconductor) [8-10]. For chronic wound healing monitoring, such devices are typically packages in the form of "smart bandages". Prior works on smart bandages have shown capabilities of detecting healing stages from largely biophysical and non-specific markers such as pressure, temperature, and pH [1-3]. However, these methods lack specific bio-molecular information, yet there is extensive knowledge of the roles of chemokines, cytokines, and growth factors in various stages of wound healing.

In this work, we present a CMOS-chip/nanowell based hybrid smart bandage interface that allows in-situ real-time and long-term label-free quantification of cytokine release from skin directly on complex wound fluids. We monitor specific cytokine binding kinetics on nanowell surface through impedance spectroscopy controlled by the custom CMOS chip. A co-design of the nanowell sensor and the CMOS chip achieves ELISA-level sensitivity demonstrating quantitative analysis of IL-6 released, and monitoring of wound healing stages over a period of two weeks from mouse wound fluids. Collectively, this allowed for the first smart bandage capable of detecting sub-pM levels of cytokine target concentrations in complex wound fluids in-situ, with high correlation to the standardized ELISA tests.

MATERIALS AND METHODS

Nanowell Sensor Fabrication

The general fabrication procedure of the nanowell sensor follows prior works [4-5]. Here, fused silica is chosen as the sensor substrate. As illustrated in Fig. 2, multiple layers of metal and insulation oxide are located in each nanowell. In general, the fabrication procedure can be summarized as follows: 1) a 5 nm thickness of chromium is sputtered as the adhesive layer followed by 150 nm of gold deposition on the fused silica substrate. 2) Standard liftoff procedures are followed by a 40 nm aluminum oxide through atomic layer deposition (ALD). 4) The second layer of electrode (again 5 nm chromium and 150 nm gold) is patterned on top of aluminum oxide by following step 1) and 2). 5) A final aluminum oxide layer is deposited through ALD on top of all electrodes to confine the electric field excitation within the nanowells. This can reduce the area for non-specific binding and selectively control the immobilized antibodies in the nanowells.

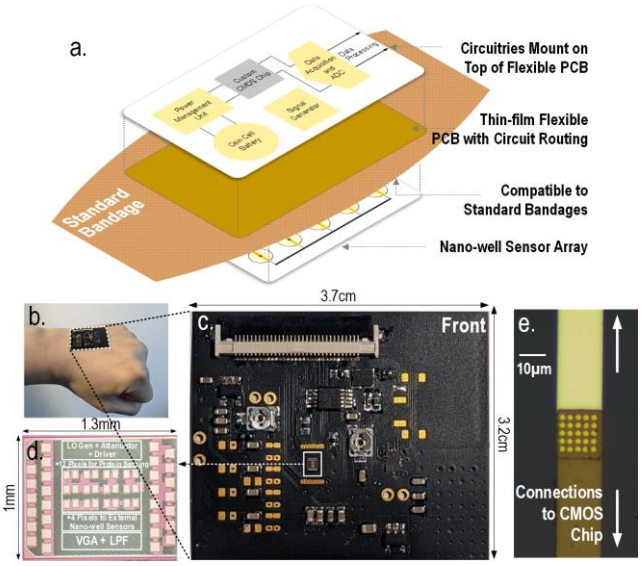

Figure 1. a) and b) CMOS/nanowell hybrid smart bandage. c) Flexible PCB with the custom silicon chip d) Micrograph of the custom-designed CMOS IC in a 65nm CMOS process. e) Microscopic photograph of nanowell sensor.

As shown in Fig. 2, an overlapping area of 20 × 20 µm^2 is separated by aluminum oxide to generate a current path to analyze the solution inside the nanowell. The two layers of the metals are

978-1-940470-04-7/HH2022/$25©2022TRF
DOI 10.31438/trf.hh2022.28

routed externally and can be eventually wire-bonded to the back of the flexible board.

Finally, a thin layer of PDMS (~ 500 um) with an opening area of 5 mm is attached to the surface of the substrate through covalent bonding after treatments in oxygen plasma chamber [4-5]. The purpose of the PDMS well is to confine the wound fluid liquid for more consistent incubation. The final assembled sensor is shown in Fig. 1, along with a microscopic photograph of the nanowell.

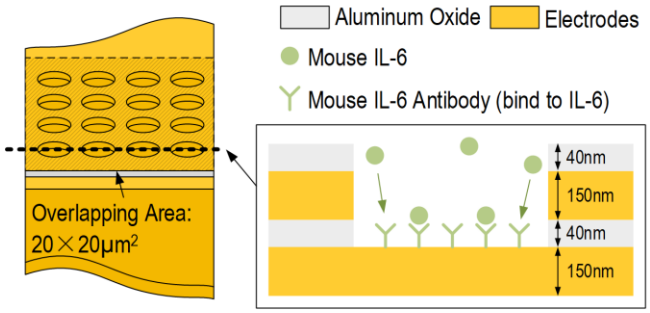

Figure 2. Cross-sectional view of the nano-well sensor, showing mouse IL-6 protein binding to IL-6 antibody resulting in impedance change between electrodes.

Mouse Wound Fluid Collection Procedure

Wound samples from mice were collected according to a protocol approved by the Institutional Animal Care and Use Committee (IACUC) at Rutgers University. The samples were collected post-surgery from the dorsal skin on a 10-week old mouse (Fig. 4). In summary, the mice were anesthetized by isoflurane one day prior to surgery. On the day of surgery, the mice were scrubbed with betadine and 70% ethanol three times followed by a biopsy punch (Integra LifeSciences; Princeton, New Jersey) to create a wound size of roughly 10 mm in diameter on mice dorsal skin. The wound is then covered with Tegaderm dressing to protect from infection.

During the wound fluid collection on day 3, 7, and 10, Tegaderm dressing is removed and dropped in a tube containing 1 mL of 1x PBS buffer solution. The tube is then centrifuged to collect the supernatant that is used for wound fluid sample for later measurements. Fig. 4 illustrates the wound closure dynamics of the mouse dorsal skin on days 3, 7, and 10 respectively.

SYSTEM ARCHITECTURE

Impedance Sensing Architecture

The impedance sensing circuit on-chip is designed and fabricated in TSMC 65 nm LP process and is based on direct-conversion sensing architecture as presented in prior works [6-7]. To sense this complex impedance change in nanowells, the CMOS chip excites the nanowell sensor at 700 kHz with 50 mVpp amplitude. The sensed current is processed on-chip with integrated trans-impedance amplifier. The amplified signal is then down-converted through in-phase (I) and quadrature (Q) clock to DC analog voltages that is low-pass filtered (10 kHz) to remove higher orders of harmonics to acquire the impedance information.

Nanowell Impedance Sensing

To better understand the EIS sensing mechanism in nanowell, an equivalent circuit model of the nanowell has been shown in Fig. 3, where R_s is the bulk fluid resistance, C_{DL} is the double-layer capacitance and R_p is the polarization resistance. The operating frequency of the impedance analysis of the nanowell sensor has been experimentally proven to be the best between 500 kHz to 1 MHz to prevent the non-ideal inductive effect of metal traces (existing at higher frequencies beyond 1 MHz), while capable of penetrating the double-layer capacitance (C_{DL}) for the sensor to tap into the protein binding events [4]. As shown in Fig. 2 and 3, when the cytokine binds to the nanowell sensor surface with immobilized probe antibody of mouse IL-6, it blocks the ion transfer in the double-layer inside the nanowells that lead to an impedance increase from the binding event [4-5]. An increase in impedance translates to a decrease in current after the nanowell channel is excited with voltage. Finally, the change in current can be captured by the on-chip TIA (Fig. 5), resulting in a positive signal.

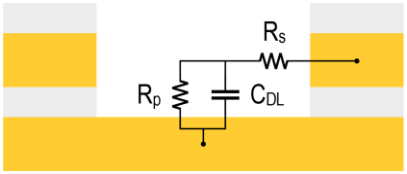

Figure 3. An equivalent circuit model inside the nanowell, showing the polarization resistance (R_p), double-layer capacitance (C_{DL}), and bulk fluid resistance (R_s).

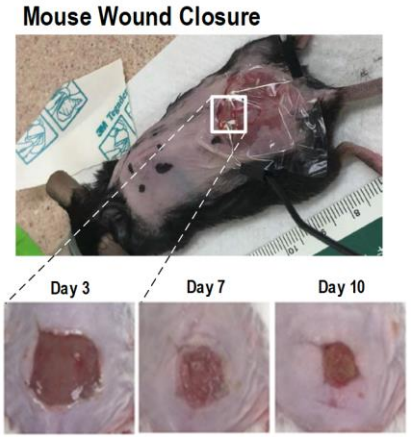

Figure 4. Mouse wound fluid collection with wound closure dynamics on day 3, 7 and 10.

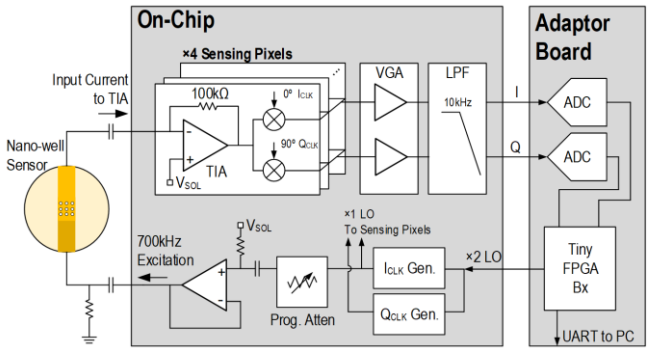

Figure 5. CMOS direct conversion transmitter/receiver architecture for impedance spectroscopy for label free detection of cytokines in complex wound fluids.

Smart Bandage Packaging

Fig. 1 illustrates the envisioned smart bandage with electronic circuits mounted on top. The nanowell sensor is located at the back to avoid obtrusion to skin. Fig. 1 shows the CMOS/nanowell cytokine sensing system on a flexible PCB with a dimension of 3.7 × 3.2 cm^2 compatible with the bandage form factor. The front side is mounted with a multi-channeled CMOS impedance spectroscopy receiver along with peripheral modules that offer power management, signal generation, and data acquisition. On the back of the sensor, we offer connections to the two electrodes of the nanowell sensors.

In addition, we choose to design an adaptor board in the prototyped system to control and monitor signal processing. The adaptor and the flexible board are communicated through a ribbon cable. In the adaptor board, we implemented a sigma-delta ADC (MCP3564, Microchip) and an FPGA (tinyFPGA BX) for data acquisition and communication to PC through UART protocol. We also implemented an LCD display panel and push buttons for easier user interface.

Ideally, all functionalities shall be implemented on a battery-powered flexible smart bandage with built-in wireless data communication. Here, we demonstrate the core functionalities of cytokine protein detection for wound healing monitoring in a wired system setup.

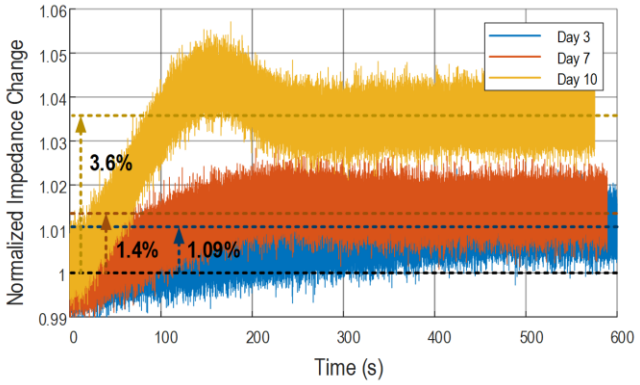

Figure 6. Real-time impedance impedance measurement of the CMOS/nanowell smart sensor showing varying normalized impedance of 3.5%, 1.4% and 1.09% at steady state in collected would sample fluid (containing cytokine IL-6) at day 3, 7, and 10 of the wound healing stages.

MEASUREMENT RESULTS

CMOS/nanowell Mouse IL-6 Cytokine Measurement Results

The measurements of the collected wound fluid sample start by diffusing 5 µL mouse IL-6 antibody to the nanowell sensor with 20 µL 1X PBS buffer solution pre-stabilized in the nanowell sensor to emulate the physical environment [4]. After the antibody diffusion to the nanowell, an additional 20 µL of 1× PBS buffer is added. This procedure is to eliminate any signal variations due to the addition of PBS buffer [4]. Finally, 5 µL of collected wound fluid is added and the complete impedance variation is recorded against time.

Fig. 6 shows the normalized impedance amplitude variation of the nanowell sensor measured at 700 kHz of excitation after the 5 µL wound fluid is added. We record the normalized impedance change of 3.6, 1.4, and 1.09% at steady state (of roughly ~10 min of signal recording) for wound fluid samples collected from days 3, 7, and 10 respectively. We then performed four trial measurements for each collected sample and the results are summarized in Fig. 7.

The steady-state impedance demonstrates the varying concentrations of cytokine release from the day of incision to final healing. As Fig. 7 shows, the cytokine release is the highest on day 3 and then slowly declines as the wound goes through the normal progression of inflammation, proliferation, and maturation.

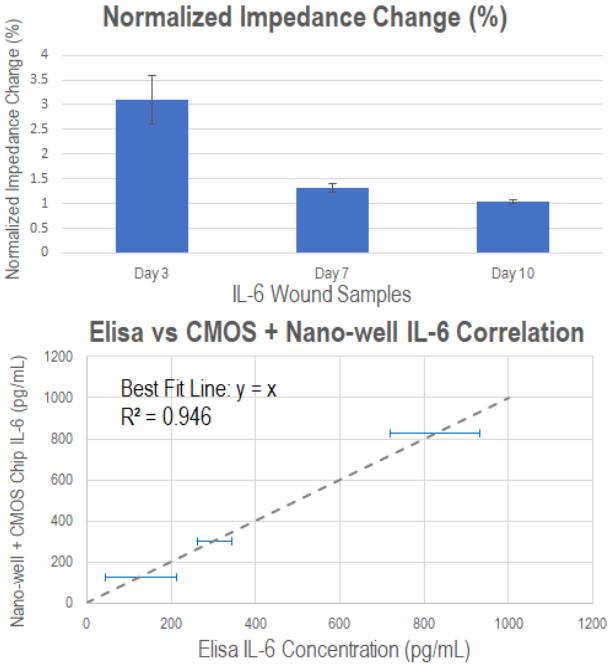

Figure 7. Measured IL-6 release profile in the mouse wound fluid (as measured with the smart bandage) showing decrease in cytokine release as the wound progress towards healing (top). A correlation plot of IL-6 measured in wound fluids with the CMOS/nano-well against a standard ELISA measurement, demonstration high correlation factor of $R^2 = 0.946$ (bottom).

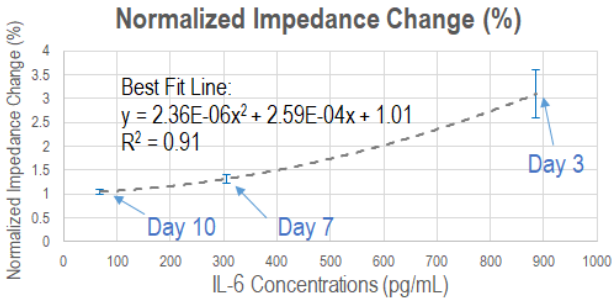

Figure 8. A best-fit line used to find the correlation between the normalized impedance and ELISA measurement results of the mouse wound fluid.

Comparisons and Correlations to ELISA Tests

In addition, we compared our results to standardized ELISA tests of IL-6 in the collected wound fluids. The IL-6 ELISA tests were performed in a commercial assay (INITROGEN, Thermo Fisher Scientific, USA) by following protocols from the manufacturer. The fluorescent absorbance is recorded using a plate reader at 450 nm wavelength to characterize the IL-6 cytokine concentration which is used for later studies on the correlation to the IL-6 measurements using the CMOS-nanowell sensor.

As shown in Fig. 8, $y = 2.36\times10^{6}\ x^2 + 2.59\times10^{-6}\ x + 1.01$ is used as the best-fit line for the CMOS-nanowell measurements.

Table 1: Comparisons with other state-of-the-art "Smart Bandages" for chronic wound healing monitoring

	This Work	A. Pal et al. [3]	M. Farooqui et al. [2]	P. Mostafalu et al. [1]
Dimensions	**3.7 × 3.2 cm²**	3.8 × 1 cm² (Estimated)	3.8 × 1 cm² (Estimated)	3 × 2 cm²
Sensing Modelities	**Impedance spectroscopy**	Chronoamperometry (Potentiostat), impedance spectroscopy (pH) and pressure.	Capacitive (CDC)	Temperature, potentiometry (pH) and heater-based drug release.
IC Chip	**Custom designed CMOS chip**	LMP9100 (potentiostat), AD5933 (impedance)	LC717A00AJ (CDC)	N.A.
Process/Manufacturer for IC Chip	**Custom Chip TSMC 65 nm LP**	TI, ADI	On Semi	N.A.
Electrode Implementations	**Nanowell sensor on glass substrate**	3 electrode configuration for pH. Omniphoic paper-based capatcitive sensor (OPSBs) for capacitive sensor (OPSBs).	Carbon ink electrodes on kapton tape	Heater electrodes on parylene substrate. Carbon/PANI, and silver electrodes on PET substrate.
Biomarker/Sensing Target	**Cytokine (IL-6)**	pH (Impedance); Uric acid (potentiostat)	Blood and pressure (CDC)	pH
Calibration /Correlation	**ELISA**	Impedance calibrated with standard pH measurement.	Pressure calibrated	Temperature and PH Calibrated.
Protein Sensing Capability	**Yes**	No	No	No
Minimum Measured Concentration /Sensitivity	**100 pg/mL**	0.2 mM (Uric acid/potassium ferricyanide)	10μL blood ~0.5pF	~50 mV/pH

Finally, the correlation between the CMOS-nanowell and ELISA is plotted in Fig. 7, showing a very high correlation to the ELISA assay, with $R^2 = 0.946$. This result demonstrates a highly reliable label-free cytokine protein sensing system for wound healing monitoring applications in a bandage form.

Finally, the performance of the CMOS-nanowell smart bandage system is summarized in Tab. 1 and compared against other state-of-the-art smart bandage systems from prior works. This work shows, for the first time, a miniaturized smart bandage system with bio-molecular sensing capability to detect cytokine concentration from the mouse wound fluids, reaching L.O.D. of ≈ 100 pg/mL of IL-6 cytokine concentration.

CONCLUSION

In summary, this work has shown, for the first time, a CMOS-nanowell sensor system that is co-designed for chronic wound healing monitoring applications. Specifically, we demonstrate IL-6 cytokine measurements from the collected mouse wound fluids. In addition, normalized impedance sensing results showed high correlation to standardized ELISA tests, demonstrating the reliability of the proposed smart bandage sensing system. The proposed system can also be easily implemented to adapt to other cytokines such as TNF-α to allow multiplexed measurements for better wound healing prediction. This hybrid approach shows a path towards highly multiplexed, low-power, compact, and low-cost smart bandages for autonomous closed-loop wound monitoring and healing devices.

ACKNOWLEDGEMENT

The authors would like to thank DARPA BETR Program for the funding support.

REFERENCES

[1] P. Mostafalu, et al., "Smart bandage for monitoring and treatment of chronic wounds," *Small*, vol. 14, no. 33, p. 1703509, 2018.

[2] M. F. Farooqui and A. Shamim, "Low cost inkjet printed smart bandage for wireless monitoring of chronic wounds," *Scientific Reports*, vol. 6, no. 1, 2016.

[3] A. Pal, D. Goswami, H. E. Cuellar, B. Castro, S. Kuang, and R. V. Martinez, "Early detection and monitoring of chronic wounds using low-cost, omniphobic paper-based smart bandages," *Biosensors and Bioelectronics*, vol. 117, pp. 696–705, 2018.

[4] P. Xie et al., "Real Time Cytokine Quantification in Wound Fluid Samples Using Nanowell Impedance Sensing," *2021 21st International Conference on Solid-State Sensors, Actuators and Microsystems (Transducers)*, 2021.

[5] S. R. Mahnoodi et al., "Single-step label-free nanowell immunoassay accurately quantifies serum stress hormones within minutes" *Science Advances*, vol. 7, no. 27, 2021.

[6] C. Zhu, et al., "CMOS-Based Electrokinetic Microfluidics With Multi-Modal Cellular and Bio-Molecular Sensing for End-to-End Point-of-Care System," *IEEE Transactions on Biomedical Circuits and Systems*, 2022, vol.15, no.6, 2021.

[7] C. Zhu et al., "18.2 CMOS-Driven Pneumatic-Free Scalable Microfluidics and Fluid Processing with Label-Free Cellular and Bio-Molecular Sensing Capability for an End-to-End Point-of-Care System," *2021 IEEE International Solid- State Circuits Conference (ISSCC)*, 2021.

[8] C. Zhu, et al., "A packaged ingestible bio-pill with 15-pixel multiplexed fluorescence nucleic-acid sensor and bi-directional wireless interface for in-vivo bio-molecular sensing," *2020 IEEE Symposium on VLSI Circuits*, 2020.

[9] L. Hong, et al., "Nano-Plasmonics and electronics co-integration in CMOS enabling a pill-sized multiplexed fluorescence microarray system," *Biomedical Optics Express*, vol. 9, no. 11, p. 5735, 2018.

[10] L. Hong, et al., "Fully integrated fluorescence biosensors on-chip employing multi-functional Nanoplasmonic optical structures in CMOS," *IEEE Journal of Solid-State Circuits*, vol. 52, no. 9, pp. 2388–2406, 2017.